Effect of the paramagnetic to spin-glass phase transition on the fundamental absorption edge of $MnIn_2Se_4$ magnetic semiconducting compound

V. Sagredo[a], T. E. Torres[b], G.E. Delgado[c], and C. Rincón[d,*]
[a]*Laboratorio de Magnetismo, Departamento de Física, Facultad de Ciencias, Universidad de Los Andes, Mérida 5101, Venezuela.*
[b]*Instituto de Nanociencia de Aragón & Laboratorio de Microscopias Avanzadas, Universidad de Zaragoza, C/Mariano Esquillor s/n, CP 50018, Zaragoza, Spain.*
[c]*Laboratorio de Cristalografía, Departamento de Química, Facultad de Ciencias, Universidad de Los Andes, Mérida 5101, Venezuela.*
[d]*Centro de Estudios de Semiconductores, Departamento de Física, Facultad de Ciencias, Universidad de Los Andes, Mérida 5101, Venezuela.*

Received 1 August 2018 ; accepted 21 September 2018

The temperature dependence of the indirect and direct fundamental band gaps of the layered compound $MnIn_2Se_4$, that crystallizes in a rhombohedral defect structure with space group $R\bar{3}m(D^5_{3d})$, was studied by optical absorption spectra. The data were analyzed in terms of current theoretical models that take into account the contribution of antiferromagnetic exchange interaction between spins to the shift of the energy gap E_G with T in the vicinity of the critical paramagnetic to spin-glass phase transition. It was established that short- and long-range effect spin correlations dominate the contribution to this shift in the critical region below about 20 K, near the spin-glass freezing temperature T_f, and noncritical one, between about 70 and 160 K, far from T_f, respectively. An intermediate temperature region, compatible with the behaviour expected for a cluster-glass transition where a gradual freezing of the magnetic moments occurs, was also observed.

Keywords: Semiconductors; electronic band structure, exchange and superexchange; order-disorder effects.

PACS: 71.20.Nr; 75.10.Nr

1. Introduction

The family of ordered-vacancy compounds (OVC's) with the general formula Mn $\square B^{III}_2 X^{VI}_4$, with B: Al, Ga or In; and X: S, Se, or Te, where $\square$ symbolizes a cation vacancy, or simply $MnB^{III}_2X^{VI}_4$, has received considerable interest in the last three decades [1-12]. These magnetic compounds, which have three metal cations (one Mn and two B's) around each anion site (X) while the fourth empty site forms an ordered array of vacancies, could exist in different crystal structures and have shown several notable physical and chemical properties associated with the crystallographic ordered array of these vacancies. In addition, the presence in these OVC's of magnetic Mn^{+2} ions make them of great interest from the point of view of their magneto-optical properties. Thus, magnetic properties of $MnIn_2Te_4$, $MnGa_2Se_4$, $MnIn_2Se_4$; which crystallize in tetragonal defect-chalcopyrite (space group $I\bar{4}2m$) [2,3], defect-thiogallate (s. g. $I\bar{4}$) [7], and cubic spinel (s. g. $Fd\bar{3}m$) [12] structures at ambient conditions, respectively, and its alloys, have been studied in detail for several authors [2-8,13-15]. $MnIn_2Se_4$, a member of this family which crystallizes in a layered rhombohedral structure (s. g. $R\bar{3}m$) [16,17], has also been studied with considerable interest. Measurements of magnetic susceptibility as a function of temperature show antiferromagnetic behavior with paramagnetic Curie temperature of about -96 K and the formation of spin-glass-like phase below about 3.6 K [6,14,15]. The occurrence of this spin-glass transition is confirmed by ac in-phase magnetic susceptibility measurements close to the spin freezing transition [14]. Here, the typical downward shift in the freezing temperature T_f, when the frequency is decreased, was observed. The zero-frequency transition temperature is $T_f = (3.58 \pm 0.02)$ K. On the other hand, analysis of its optical absorption coefficient spectra [1,18] reveals that the lowest-energy-gap of this compound is indirect between parabolic bands that vary from 1.55 to 1.43 eV in the temperature range from 10 K to 295 K [18]. This indirect band-to-band transition arises from the uppermost $\Gamma_4(z)$ valence band at Γ point, to the conduction band minimum located at a lower-symmetry point different from Γ [12]. Additionally [18], two direct band-to-band transitions, beginning at 1.72 and 1.85 eV, at 295K, and at 1.82 and 1.96 eV, at 10 K, from the uppermost $\Gamma_4(z)$ heavy-hole and middle $\Gamma_5(z)$ light-hole bands, to the $\Gamma_1(s)$ conduction band, were observed in the high energy region. At energies around 2.2 eV, an internal transitions from $^6A_1$ ground state to the $^4T_1$ d-excited level of Mn^{+2} ion, was also observed from photoluminescence spectra.

A semiconductor property which is affected by the presence of Mn^{+2}, especially at low temperatures, is the band gap E_G. Theoretical studies have shown [19,20] that nearby a critical point, as for example the spin glass transition temperature T_f, a magnetic contribution to the variation E_G with temperature, due to the exchange interaction between the d electrons of Mn^{+2} ions and the electrons in the valence and conduction bands, should occur. For antiferromagnetic exchange interaction, as is the case of $MnIn_2Se_4$, an increase in E_G around T_f is expected [19]. In spite of these advances, to

the best of our knowledge, a detailed study of the temperature dependence of E_G for semiconductors where a paramagnetic to spin-glass transition occurs, has not been reported. This is of interest in relation to whether it is a true phase transition from a thermodynamic point of view or a gradual freezing of the magnetic moments. For this reason, in the present work we present a study of the temperature dependence of the fundamental band gaps in $MnIn_2Se_4$. This dependence is discussed in terms of the theoretical models reported in the literature that analyze the magnetic contribution to the shift of E_G with T.

2. Crystal growth and experimental details

Bulk single-crystals of $MnIn_2Se_4$ were grown by chemical vapor transport technique from polycrystalline $MnIn_2Se_4$ which was synthesized from stoichiometric amounts of 5 N pure Mn, In, and Se, in an evacuated and closed ampoule. This was carried out by gradual heating of the mixture, subsequent melting, and gradual cooling through the freezing point. For the crystal growth, a 20 cm long and 1.5 cm inner diameter quartz stationary ampoule loaded with 1.5 g charge of the pre-synthesized material was used. I_2, with a concentration of 4 mg/cm^3 of ampoule volume, was employed as transport agent in the reaction. The transport reaction was carried out in a two-temperature zone furnace during seven days between 800°C, in the highest-temperature region of the ampoule where the source pre-reacted material is initially placed, and 750°C, in the lowest-temperature region where the obtained bulk crystals are deposited. As-grown bulk crystals have typical dimensions of about 20-30 mm^2 and show a dark color.

A SIEMENS D-5005 diffractometer, operated at 30 kV and 15 mA, with a Cu-target ($\lambda-$Cu Kα = 0.15418 nm) tube, a graphite monochromator and a scintillation detector, was used to register the powder X-ray diffraction pattern at room temperature. The intensity data were recorded in a θ/θ reflection mode from 10 to 100° with a step size of 0.02° and a scan speed of 25 s/step. Quartz was used as an external standard.

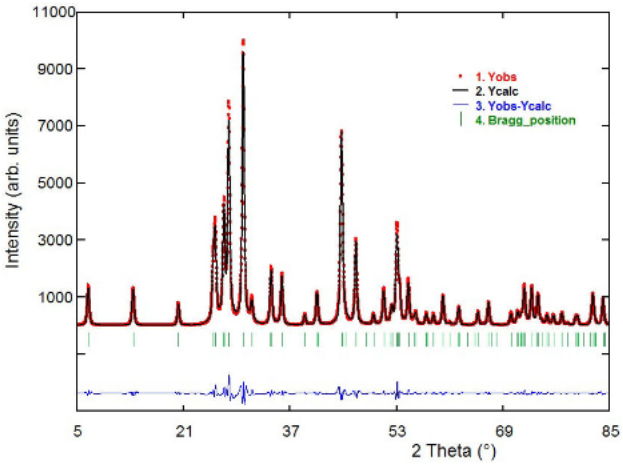

FIGURE 1. Observed (circles), calculated (solid line), and difference plot of the final Rietveld refinement of $MnIn_2Se_4$.

The absorption coefficient spectra α was obtained from the optical transmittance T_r spectra through the relation [21] $T_r = [(1-R)^2\exp(-\alpha x)]/[1-R^2\exp(-2\alpha x)]$, where x is the thickness sample and $R \approx 0.223$ [18], is the reflectivity. T_r spectra were measured by using an Acton Research Spectra P-500 spectrometer in the energy range from 1.2 to 2.4 eV. For the measurements of these spectra at various temperatures from 10 to 295 K, the samples were mounted on a cold finger of a Janis closed cycle refrigerator.

3. Powder X-ray diffraction analysis

To determine the crystal structure and unit cell parameters of $MnIn_2Se_4$, powder X-ray diffraction analysis was carried out. The structure was refined by means of the Rietveld method using the Fullprof program. For the refinement, atomic coordinates of $MnIn_2Se_4$ single-crystal reported by Range *et al.* [17], where used in the analysis. The Rietveld plot is shown in Fig. 1. The final refinement converged to the profile agree-

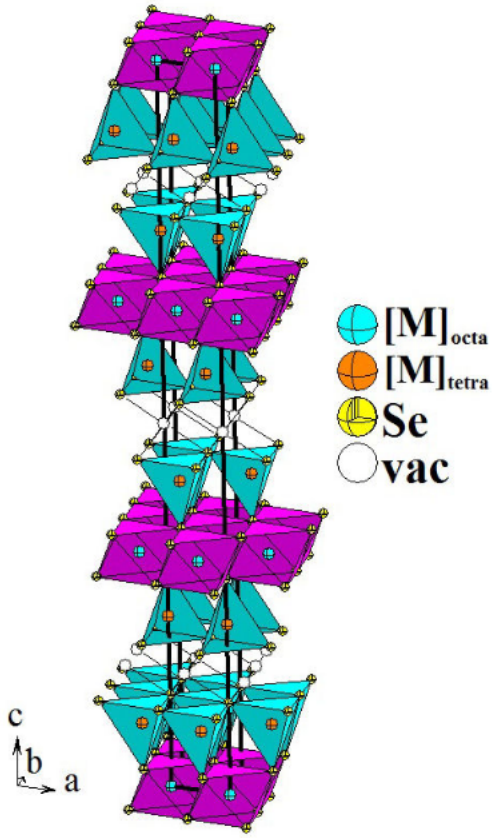

FIGURE 2. The rhombohedral structure of $MnIn_2Se_4$ with octahedral (purple) and tetrahedral (green) polyhedra. Mn, In, Se atoms and cation vacancies, are represented by green, orange, yellow and white spheres, respectively.

TABLE I. Unit cell parameters a, c, and c/a, reported in the literature for $MnIn_2Se_4$.

Compound	Structure	a (nm)	c (nm)	c/a	Ref
$MnIn_2Se_4$	Rhomboedral (space group: $R\bar{3}m$)	0.4051(1)	3.9464(2)	9.74	[16]
		0.405(6)	3.94(9)	9.73	[17]
		0.4055(1)	3.9467(2)	9.733	Present work

ment factors: $R_p = 9.9$ %, $R_{wp} = 10.5$ %, $R_{\text{exp}} = 9.1$%, $S = 1.2$. $MnIn_2Se_4$ crystallizes in the centrosymmetric space group $R\bar{3}m(D^5_{3d})$, $Z = 3$, with unit cell parameters: $a = 0.4055(1)$, $c = 3.9467(2)$ nm, $c/a = 9.733$, and $V = 0.5620(2)$ nm^3. These values are in good agreement with those reported in [16,17] and also shown in Table I.

The crystallographic analysis confirms that $MnIn_2Se_4$ belongs to a rhombohedral defect structure with tetrahedral and octahedral cation-to-anion coordination, which can be expressed by the chemical formula $[M]_{oct}([M]_{tetr})_2Se_4$, where [M] means either Mn and In cations distributed in a disordered arrangement. $[M]_{oct}$ being the disordered cations occupying the octahedral sites, six-fold coordinated by Se anions, while $[M]_{tetr}$ being these cations occupying the tetrahedral sites, four-fold coordinated by Se anions.

The unit cell diagram of $MnIn_2Se_4$ is shown in Fig. 2. A close-packed Se layer, with Mn and In cations at random in octahedral and tetrahedral voids, leaving the interlayers between h-stacked layers vacant, can be observed in this figure.

4. Temperature dependence of the band gap energy

The nature of the fundamental absorption edge in $MnIn_2Se_4$ was examined by us in a previous article [18] by studying the optical absorption coefficient spectra α_c of this compound at several temperatures between 10 and 295 K. It was found, at values of α_c lower than about 2×10^3 cm^{-1}, that the lowest energy gap is indirect. On the other hand, for values of α_c greater than 2×10^3 cm^{-1}, the absorption coefficient spectra show the presence of two direct band-to-band transitions at higher energies. These two processes, with characteristic energies E^I_{GD} and E^{II}_{GD}, correspond [18] to direct transitions from the uppermost $\Gamma_4(z)$ and the middle $\Gamma_5(z)$ valence bands, to the $\Gamma_1(s)$ conduction band of $MnIn_2Se_4$, respectively.

The shape of E_G vs. T curve in non-magnetic semiconductors is approximately flat at low temperatures, but smoothly changes to a linear decrease in the high temperature region. However, as can be seen in Fig. 3, where the temperature variation of E_{GI}, E^I_{GD} and E^{II}_{GD} energy gaps of $MnIn_2Se_4$ in the form of solid circles are plotted, this is not observed in the present case where going to low temperatures, the curves also shown a nearly linear variation with T.

Such a behavior at low T, which has also been observed in other materials having antiferromagnetic exchange [22-24], is also consistent with the theoretical study [19] about the effects of spin fluctuations on the shift of the E_G with temperature around a magnetic critical temperature T_C. According to this study, for an antiferromagnetic exchange interaction between spins, a magnetic contribution is expected that should cause an increase ΔE_{GM} in the band gap of the semiconductor in the vicinity of the spin-glass transition temperature T_f.

To describe the behavior of E_G near the critical freezing temperature T_f in terms of a power law, the reduced temperature difference $\tau = |T - T_f|/T_f$, which is zero at the phase transition, is introduced in the analysis of the data [19]. For a semiconductor with antiferromagnetic exchange interaction, the theory indicates that ΔE_{GM} satisfies a relation of the form

$$(d/d\tau)\Delta E_{GM} = -A\tau^{-\lambda} \tag{1}$$

where λ is the critical exponent of the band-gap variation ΔE_{GM} and A is a parameter that measures the strength of the total spin interaction on this variation.

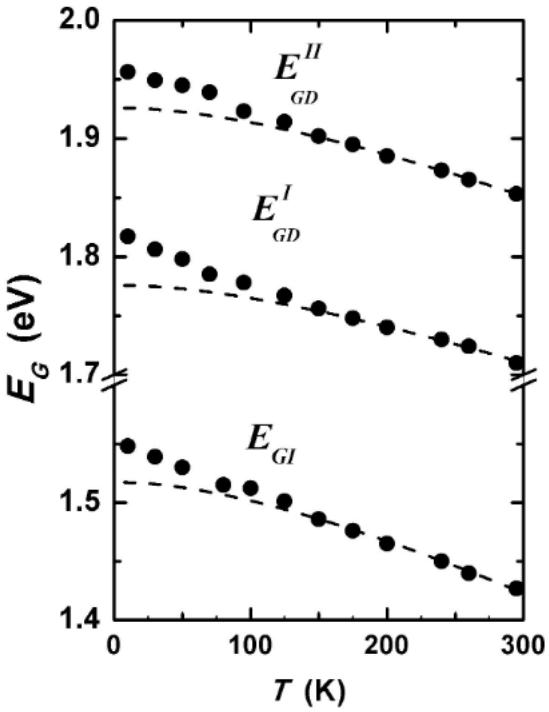

FIGURE 3. Temperature variation of E_{GI}, E^I_{GD} and E^{II}_{GD} energy gaps of $MnIn_2Se_4$. Solid circles (•) and broken lines represent the experimental points and the fit to the experimental curves in the high-temperature region ($T > 150$ K) by using Eq. (5), respectively.

Two different temperature regions should be taken into account in this analysis. The critical region, near the spin-glass freezing temperature T_f, where the main contribution to ΔE_{GM} vs. T arises from short-range spin correlations, and the non-critical one, far from T_f, ($T > Tf$) where longer-range effects turn out to be important. Kasuya and Kondo [25], when studying the anomalies of the electrical resistivity in antiferromagnetic materials that exhibit order-disorder second-order phase transitions, have found that in the critical region λ is equal to the critical index of the specific heat magnetization α, which has a value close to zero. On the other hand, for τ outside the critical region (at $T > T_f$), Alexander *et al.* [19] predict that the value of exponent λ should be 1/2. Analyses of experimental E_G vs. T data for various diluted magnetic semiconductors showing antiferromagnetic behaviour [22-24] confirm the predictions of both these models.

In order to obtain a theoretical expression for ΔE_{GM} that can be compared with the data, Eq. (1) should be integrated.

$$\Delta E_{GM}(\tau) = -A\tau^{1-\lambda}/(1-\lambda) + c \qquad (2)$$

then, if the value of ΔE_{GM} at T_f is expressed as ΔE_f, the constant of integration C in Eq. (2) can be removed and this equation can be written as:

$$\Delta E_{GM}(\tau) - \Delta E_f = -A\tau^{1-\lambda}/(1-\lambda) \qquad (3)$$

Eq. (3) can be written as

$$-\ln[\Delta E_{GM}(\tau) - \Delta E_f] = (1-\lambda)\ln\tau + \ln[A/(1-\lambda)]. \qquad (4)$$

Thus, values of the magnetic shift ΔE_{GM} determined from the experimental data can be analyzed in terms of Eq. (4). To calculate ΔE_{GM} it is necessary to know the values of E_G in the absence of any magnetic effects. These can be determined by extrapolating to low temperatures the $E_G(T)$ curves at high temperatures where the magnetic effects are unimportant. This may be done by using the expression for the E_G vs T variation based on Bose-Einstein phonon model, given by [26]

$$E_G(T) = E_B - a_b\{1 + 2[\exp(\Phi/T) - 1]^{-1}\}, \qquad (5)$$

where $E_B - a_b = E_G(0)$ is the value of the energy gap at 0 K, and Φ an average phonon related to the Debye temperature.

The difference between the measured curves and those extrapolated by using Eq. (5) is thus attributed to the magnetic contributionΔE_{GM}. Hence, the data shown in Fig. 3 have to be fitted to Eq. (5) in the high-temperature region ($T \geq 150$ K). Thus, in order to reduce the number of the free parameters to be determined from the data, *i.e.* E_B, a_B, and Φ, to only two, we have taken $\Phi = 200$ K, which is the Debye temperature for $MnIn_2Se_4$ estimated from its melting point ($T_M \approx 1178$ K) by using the classical Lindemann expression, which relates Φ to the melting point T_M through the expression $\Phi \sim TM^{1/2}$ [27]. Hence, using $\Phi \approx 200$ K as a fixed parameter, Eq. (5) was fitted to the experimental $E_{GI}(T)$, $E^I_{GD}(T)$, and $E^{II}_{GD}(T)$ data of Fig. 3, in the temperature range from 150 to 300 K. Values of $E_G(0)$ and a_B, obtained from this fit are also given in Table II. Theoretical extrapolated $E_{GIE}(T)$, $E^I_{GDE}(T)$, and $E^{II}_{GDE}(T)$ curves, obtained from Eq. (6), are also shown in Fig. 3 by broken lines. The magnetic shift can thus be obtained as $\Delta E_{GM}(T) = E_G(T) - E_{GE}(T)$, for these three curves. The value of ΔE_G at $T_f \approx 3.6$ K for each of the curves in Fig. 3, as obtained directly from these curves, was 34, 39 and 33 meV, for $E_{GI}(T)$, $E^I_{GD}(T)$, and $E^{II}_{GD}(T)$, respectively.

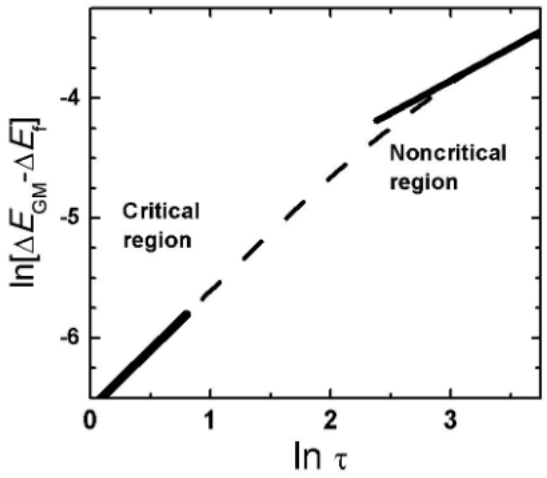

FIGURE 4. Temperature variation of ΔE_{GM} for the indirect band-to-band transition E_{GI} observed in $MnIn_2Se_4$ in the form of a plot of $\ln(\Delta E_{GM} - \Delta E_f)$ vs. $\ln\tau$, in the temperature range where the magnetic contribution to E_G vs. T is appreciable ($T < 150$ K) (broken line). The slopes in both low and high-τ regions are indicated by bold continuous straight lines.

TABLE II. Values of parameters $E_G(0)$ and a_B, obtained from the fit of $E_{GI}(T)$, $E^I_{GD}(T)$ and $E^{II}_{GD}(T)$ data of Fig. 3 to Eq. (5) using $\Phi \approx 200$ K as a fixed parameter, and λ_c, λ_{nc}, A_c and A_{nc}, obtained from the fit of $\Delta E_{GM}(\tau)$ data to Eq. (4) in the critical and noncritical regions.

Optical transition	$E_G(0)$ (eV)	a_b (eV)	λ_c	λ_{nc}	A_c (meV)	A_{nc} (meV)
E_{GI}	1.516 ± 0.001	0.044 ± 0.06	0.02	0.46	1.3	2.0
E^I_{GI}	1.775 ± 0.001	0.031 ± 0.001	0.08	0.49	1.6	2.7
E^{II}_{GI}	1.925 ± 0.005	0.035 ± 0.001	0.09	0.52	1.4	2.5

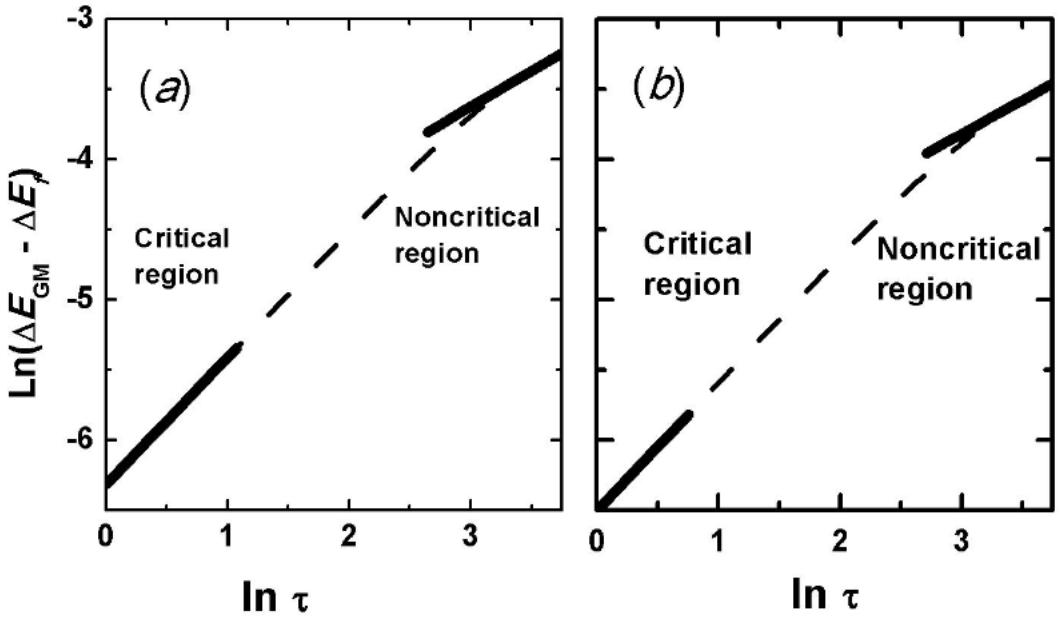

FIGURE 5. Temperature variation of ΔE_{GM} for the indirect band-to-band transition E^I_{GD} and E^{II}_{GD} observed in $MnIn_2Se_4$ in the form of a plot of $\ln(\Delta E_{GM} - \Delta E_f)$ vs. $\ln\tau$, in the temperature range where the magnetic contribution to E_G vs. T is appreciable ($T < 150$ K) (broken line). The slopes in both low and high-t regions are indicated by bold continuous straight lines

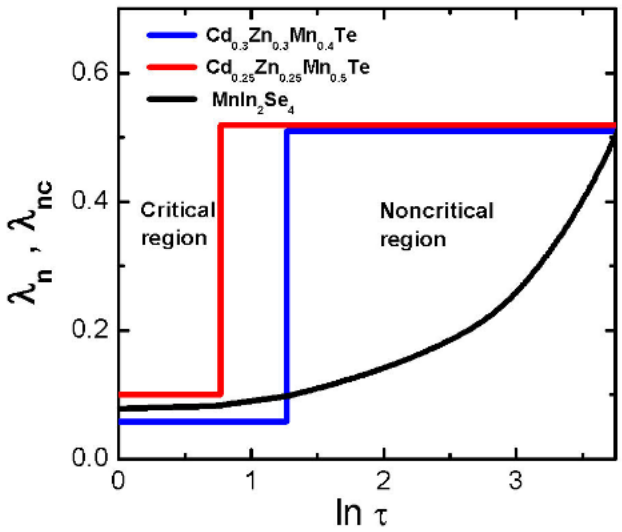

FIGURE 6. Variation of λ obtained from the slope of broken lines in Fig. 5, with $\ln\tau$ in the critical and noncritical regions for the direct transition E^I_{GD} in $MnIn_2Se_4$ (black line). Values of λ for the lowest band gap of $Cd_{0.3}Zn_{0.3}Mn_{0.4}Te$ (blue line) and $Cd_{0.25}Zn_{0.25}Mn_{0.5}Te$ (red line) $Cd_xZn_yMn_zTe$ pseudo-ternary alloys, taken from [22] are also shown.

The temperature variation of ΔE_{GM} for the three band-to-band transitions in the form of a plot of $\ln(\Delta E_{GM} - \Delta E_G)$ vs. $\ln\tau$, in the temperature range where the magnetic contribution to E_G vs. T is appreciable, is shown a broken line, in Figs. 4, 5a, and 5b, for E_{GI}, E^I_{GD}, and E^{II}_{GD}, respectively. It can be seen that in the low τ region all the curves show a linear behaviour, in good agreement with Eq. (4). The slope $(1 - \lambda)$ in this temperature region is found to be 0.98, 0.92, and 0.91 (± 0.02), for E_{GI}, E^I_{GD}, and E^{II}_{GD} curves. These give $\lambda_c \approx 0.02$, 0.08 and 0.09 for these curves, respectively. This is also shown in Table II. These values are in good agreement with theoretical analysis that predicts $\lambda \approx 0$ in the critical region [25]. In addition, in the high-τ region, the slope of the line is found to be 0.54, 0.51, and 0.48 (± 0.02). This gives $\lambda_{nc} \approx 0.46$, 0.49, and 0.52 ($\pm 0.02$) for these curves, respectively, which is also in agreement with the theory that predicts $\lambda_{nc} \approx 0.5$ in this region [19].

However, it is also observed that an intermediate temperature region exists where λ which was obtained from the slope of the broken lines at each temperature in Fig. 5, gradually increases between these two values. This is shown in Fig. 6 where the variation of λ with $\ln\tau$ is plotted for the $E^I_{GD}(T)$ optical transition. Values of λ for two alloys of $Cd_xZn_yMn_zTe$ pseudo-ternary system, a material for which a transition from antiferromagnetic-to-spin glass phase has been observed [34], are also shown in this figure for comparison.

The existence of this intermediate region, which does not appear in ideal antiferromagnetic compounds where an abrupt change when passing from critical to noncritical regions is observed [22-24], indicates that in the present case a gradual change is occurs when $MnIn_2Se_4$ pass from the spin-glass phase to the paramagnetic one. This fact reveals that it is not a true phase transition in the thermodynamic sense but a gradual freezing of the magnetic moments.

Thus, it is found that in $MnIn_2Se_4$ below about 20 K, short-range spin correlations give the main contribution to ΔE_{GM} vs. T, while longer-range effects becomes dominant at temperatures between about 70 to 150 K. In the intermediate temperature region, where λ varies from about 0.02 to

0.40, both these two spin correlation effects should be taken into account in the analysis of magneto-optical properties of this compound.

Values of the parameters A in the critical and non-critical regions, obtained from the fit are also shown in Table II. These values of A_c and A_{nc}, are in good agreement with those reported for antiferromagnetic semiconductors [22,24] that vary from 0.2 to 28.0 and 4.8 to 18.0 meV, respectively.

5. Conclusion

The temperature dependence of the indirect and direct fundamental band gaps of single crystals on the layered compound $MnIn_2Se_4$, that crystallize in the rhombohedral defect structure with space group $R\bar{3}m(D^5_{3d})$, were studied by optical absorption spectra. The data were analyzed in terms of the theoretical models by Alexander *et al*. [19] and Kasuya and Kondo [25] that takes into account the magnetic contribution to the shift of E_G with T. It is suggested that short-range effect spin correlations dominate the contribution to the shift below about 20 K, in the critical region of the paramagnetic to spin-glass phase transition, whereas longer-range effect spin correlations control the contribution to this shift in the temperature range from about 70 to 150 K, in the noncritical region. An intermediate temperature region, where a gradual freezing of the magnetic moments occurs, was also observed. This probably indicates that, from a thermodynamic point of view, the spin-glass phenomenon is a gradual freezing of the magnetic moments instead of a true phase second order transition.

Acknowledgments

This work was supported by the Consejo de Desarrollo Científico, Humanístico, Tecnológico y de las Artes (CDCHTA) de la Universidad de Los Andes, Mérida-Venezuela, under Project No. C-1658-09-65-A.

1. H. Neumann, C. Bellabarba, A. Khan, V. Riede, *Cryst. Res. Technol* **21** (1986) K21.
2. K. J. Range, and Hübner, Z. Naturf. B **30** (1975) 145.
3. G. E. Delgado, C. Chacón, J. M. Delgado, V. Sagredo, *Phys. Status. Solidi A* **134** (1992) 61.
4. M. Cannas, L. Garbato, A. G. Lehmann, N. Lampis, F. Ledda, *Cryst. Res. Technol*. **33** (1998) 417.
5. V. Sagredo, E. ter Haar, G. Attolini, *Physica B* **320** (2002) 407.
6. R. Tovar *et al., Mater. Res. Bull*. **37** (2002) 1011.
7. N. N. Niftiev, M. A. Alidzhanov, O. B. Tagiev, F. M. Mamedov, M. B. Muradov, *Semiconductors*, **38** (2004) 531-532.
8. V. Sagredo, M. C. Morón, L. Betancourt, G. E. Delgado, *J. Magn. Magn. Mater*. **312** (2007) 294.
9. F. J. Manjón *et al., Phys. Status Solidi. B* **244** (2007) 229.
10. M. C. Menard *et al., Chem. Mater.* **23** (2011) 3086.
11. B. G. Tagiev, *et al., Semiconductors*, **46** (2012) 705.
12. S. H. You, K. J. Hong, T. S. Jeong, K. Y. Lim, C. J. Youn, *J. Cryst. Growth* **404** (2014) 116.
13. M. Quintero, M. Morocoima, A. Rivero, P. Bocaranda, J. C. Woolley, *J. Phys. Chem. Sol.* **58** (1997) 491.
14. J. C. M. Ochoa *et al*, *J. Magn. Magn. Mater*, **272-276** (2004) 1308.
15. J. C. Mantilla *et al*., *J. Phys. Condens. Mat.* **17** (2005) 2755.
16. G. Doll, M. Ch. Lux-Steiner, Ch. Klock, J.R. Baumann, E. Bucher, *J. Cryst. Growth* **104** (1990) 593.
17. K.-J. Range, U. Klement, G. Döll, E. Bucher, J. R. Baumann, *Z. Naturf.* **46b** (1991) 1122.
18. C. Rincón, T. E. Torrres, V. Sagredo, S. J. Jiménez-Sandoval, E. Mares-Jacinto, *Physica B* **477** (2015) 123.
19. S. Alexander, J. S. Helman, J. Balberg, *Phys. Rev. B* **13** (1976) 304.
20. R. B. Bylsma, W. M. Becker, J. Kossout, U. Debska, D. Yoder-Short, *Phys. Rev B* **33** (1986) 8207.
21. J. I. Pankove, *Optical Properties of Semiconductors.* (Dover Pub., Inc. New York, 1971).
22. T. Donofrio, G. Lamarche, J. C. Woolley, *J. Appl. Phys.* **57** (1985) 1932.
23. M. Quintero, B. D. Marks, J. C. Woolley, *J. Appl. Phys*. **66** (1989) 2402.
24. X. L. Chen, A. M. Lamarche, G. Lamarche, J. C. Woolley, *J. Phys. Condens. Mat.* 5 (1993) 7143.
25. T. Kasuya and A. Kondo, *Solid State Commun.* **14** (1974) 249.
26. L. Viña, S. Logothetidis, M. Cardona, *Phys. Rev. B* **30** (1984)1979.
27. L. E. Shelimova and S. K. Plachkova, *Phys. Status Sol. A* **104** (1987) 679.
28. T. Donofrio, G. Lamarche, and J. C. Woolley, *J. Appl. Phys.* **57** (1985) 1937-1940.